(k, n)-Image Reversible Data Hiding

Gwoboa Horng[1], Ying-Hsuan Huang[1], Chin-Chen Chang[2,3,*] and Yanjun Liu[3,4]

[1]Department of Computer Science and Engineering,
National Chung Hsing University, Taichung 40227, Taiwan
gbhorng@cs.nchu.edu.tw; phd9807@cs.nchu.edu.tw

[2]Department of Information Engineering and Computer Science,
Feng Chia University, Taichung 40724, Taiwan
alan3c@gmail.com

[3]Department of Computer Science and Information Engineering,
Asia University, Taichung 41354, Taiwan
alan3c@gmail.com; yjliu104@gmail.com

[4]School of Computer Science and Technology,
Anhui University, Hefei, 230039, China
yjliu104@gmail.com

ABSTRACT. *Dual-images reversible data hiding methods can embed massive condential messages and generate an excellent stego image. However, each condential message and the cover image cannot be recovered if any stego image is missed. In order to overcome this drawback, we proposed a (k, n)-image reversible hiding method that can restore the cover image and k condential images from n stego images. Additionally, (n - k) cheating images can be embedded into stego images, which can deceive hackers or increase their analysis cost. Consequently, the proposed method possesses four properties, i.e., large hiding capacity, excellent stego image, good robustness and security. Experimental results show that the performances of the proposed method are better than those of recently proposed methods.*

Keywords: Reversible data hiding, Stego image, Cheating image, Hiding capacity, Robustness, Security

1. **Introduction.** Reversible data hiding can embed the encrypted confidential message into a cover image to obtain a stego image, as shown in Fig. 1. Since the stego image is very similar to the cover image, the confidential message hided in the stego image cannot be detected by a third party. When a legal user receives the stego image, the encrypted confidential message can be extracted and the cover image can be restored by using the extraction and recovery algorithm.

Reversible data hiding methods can be classified into five categories, i.e., compression-based method [3, 5], difference expansion (DE) method [1, 7, 10, 11, 12, 16, 19, 20, 22, 23, 24, 25], histogram-based method [6, 8, 9, 17, 18, 21, 26, 27, 28], reversible contrast mapping (RCM) method [2, 14] and dual-images method [4, 13, 15]. Compression-based reversible hiding methods [3, 5] extracted the least significant features of the cover image and then compressed them. Afterwards, the least significant features in the cover image were replaced by compressed results and confidential messages. Since the method only modifies the least significant features in the image, the image quality is satisfactory

However, there is a drawback in the method that when compressed results rise the embedding rate is not good. Therefore, reducing the size of compressed results has become an important issue for the compression-based method.
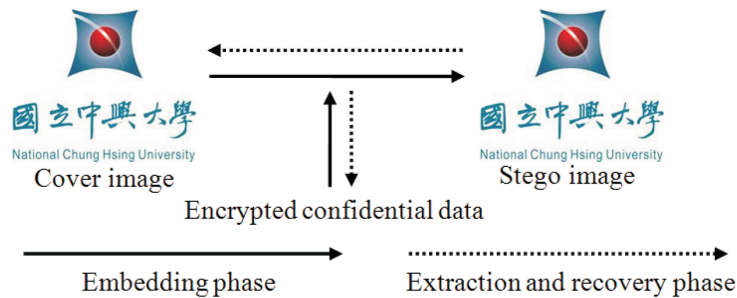

FIGURE 1. Reversible data hiding

Unlike the compression-based methods, DE-based reversible hiding methods [1, 7, 10, 11, 12, 16, 19, 20, 22, 23, 24, 25] first calculated the difference between the current pixel and its neighboring pixel and then expanded the difference by doubling it. Thus, the expanded difference became an even number. According to the embedding rule, the expanded difference was modified as odd when the confidential message is one; otherwise, the expanded difference remains unchanged when the confidential message is zero. In other words, the confidential message was embedded into the least significant bit (LSB) of the expanded difference. In the extraction and recovery phase, the confidential message can be obtained by extracting the LSB of the expanded difference. Although this approach has a high embedding rate, the expanded difference would lead to increased image distortion.

To overcome the above problem, histogram-based reversible data hiding methods have been proposed [6, 8, 9, 17, 18, 21, 26, 27, 28]. The method counted the appearance frequency of the cover pixel (or the difference between two adjacent pixels) to generate a histogram. In the histogram, the pixels with maximum and minimum appearance frequency are denoted as peak point P and zero point Z respectively. In order to create a hiding space, the pixel ranged in $[P + 1, Z]$ was increased by one. The remaining pixels keep unchanged to decrease the image distortion. However, only the pixel that equals peak point P can embed one confidential message in this method.

RCM-based reversible data hiding methods [2, 14] transformed two adjacent pixels into two integer values by using an integer transformation method. Then, the confidential message was embedded into these two values. Although the method is simpler than the above three methods, serious image distortion will occur due to the integer transformation method.

Dual-images hiding methods [4, 13, 15] are to embed the confidential message into two same cover images by using the pre-established embedding rules. In the embedding rules, the pixel was modified by only adding or subtracting one. This indicates that the stego image produced by the method has an excellent quality. Additionally, each pixel can embed one confidential message, thereby achieving a high embedding rate. However, all confidential messages and the cover image cannot be recovered if any stego image is lost.

In this paper, we proposed the (k, n)-image reversible data hiding method to solve the above problem. The proposed method can extract the confidential message and recover the cover image even if some stego images are lost. Moreover, the proposed method can maintain the advantages of dual-images reversible data hiding method, i.e., high embedding rate and excellent stego image. In order to enhance the security the proposed,

method not only embeds k confidential images but also embeds $(n-k)$ cheating images, which can increase hacker's analysis cost efficiently.

The rest of the paper is organized as follows. The proposed method and its performance are described in Sections 2 and 3, separately. The conclusions are given in Section 4.

2. (k,n)-image reversible data hiding method. Since dual-images reversible hiding method modifies pixels by only adding or subtracting one, the stego image has an excellent quality. Furthermore, massive confidential messages can be embedded into two images by using this method. However, all confidential messages and the cover image cannot be recovered if any stego image is lost. The (k,n) -image reversible data hiding method proposed in this paper can solve the above problem and keep the advantages of dual-images hiding method. Moreover, the proposed method can generate n stego images to embed k encrypted confidential images and $(n-k)$ cheating images, thereby achieving a high hiding capacity and cheating hackers.

The rest of Section 2 is organized as follows. Subsections 2.1 and 2.2 describe the embedding algorithm and the recovery and extraction algorithm, separately. Subsection 2.3 describes the solutions for overflow and underflow problems. The adopted notation of the proposed method and its definition are listed in Table 1.

TABLE 1. Notation and its definition

Notation	Definition
RS	Random seed
I	Cover image
n	Number of stego images
S^t	The tth encrypted confidential image, where $t = \{1, 2, ..., k\}$ and $2 \leq k \leq n$
C^m	The mth cheating image that includes the meaningful and meaningless messages, where $m = \{1, 2, ..., n-k\}$
W	Width of the cover image
H	Height of the cover image
$P_{i,j}$	The cover pixel with the location (i,j)
$\hat{P}_{i,j}^l$	The pixel with the location (i,j) in the lth stego image, where $1 \leq l \leq n$
$e_{i,j}^l$	The bit with the location (i,j) in the lth binary image that equals S^t or C^m
$d_{i,j}'$	The difference between the pixel with the position (i,j) of the first stego image and that of the last stego image

2.1. Embedding phase. In the proposed method, n binary images, including k encrypted confidential images and $(n-k)$ cheating images, can be hidden into n stego images by using the embedding rules and the embedding order, which is generated by a random seed RS. The flowchart of the embedding method is shown in Fig. 2.

The embedding algorithm is described as follows.

Step 1. Rearrange n binary images, i.e., k encrypted confidential images $S^t(t = 1, 2, \ldots, k)$ and $(n-k)$ cheating images $C^m(m = 1, 2, \ldots, n-k)$, according to the embedding order, which is generated by using a random seed RS. In the lth rearranged image, one bit with the location (i,j) is denoted as $e_{i,j}^l$

Step 2. Use the following three embedding rules to embed $e_{i,j}^l$ into stego pixel $\hat{P}_{i,j}^l$.

Rule 1. If the embedded messages $\{e_{i,j}^1, e_{i,j}^2, \ldots, e_{i,j}^n\}$ are all 0, then $\hat{P}_{i,j}^l = P_{i,j}$
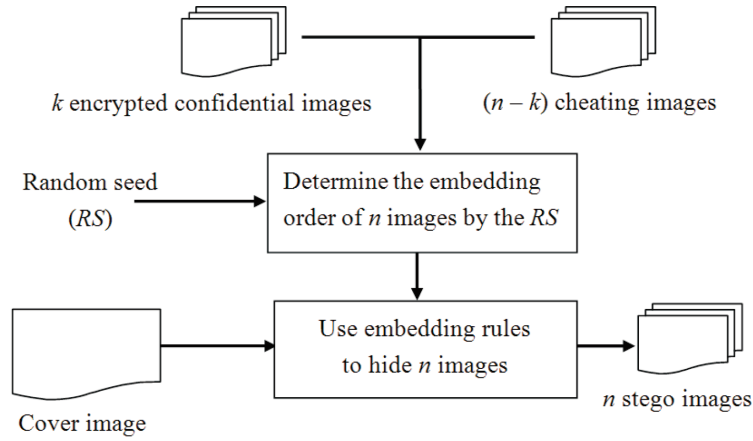
FIGURE 2. Flowchart of the embedding method

Rule 2. If the embedded messages $\{e_{i,j}^1, e_{i,j}^2, \ldots, e_{i,j}^n\}$ are all 1, then $\hat{P}_{i,j}^1 = P_{i,j} - 1$, $\hat{P}_{i,j}^n = P_{i,j} + 1$ and $\hat{P}_{i,j}^l = P_{i,j}(l = 2, 3, \ldots, n-1)$.

Rule 3. If the embedded messages $\{e_{i,j}^1, e_{i,j}^2, \ldots, e_{i,j}^n\}$ consist of 0 and 1, then $\hat{P}_{i,j}^l = P_{i,j} + e_{i,j}^l (l = 1, 2, \ldots, n)$

Since each pixel can embed one message, the ideal hiding capacity is $W \times H \times n$. It is indicated that our hiding capacity will approach infinity if the number of stego images approaches infinity.

In the embedding phase, the pixel does not need to be modified if the embedded message $e_{i,j}^l$ is 0. Otherwise, if the embedded messages $\{e_{i,j}^1, e_{i,j}^2, \ldots, e_{i,j}^n\}$ are all 1, only two pixels (i.e., $\hat{P}_{i,j}^1$ and $\hat{P}_{i,j}^n$) need to be modified by adding or subtracting one according to Rule 2. The pixels that need to be modified by Rule 3 are more than those by Rules 1 and 2, but each of them is only increased by one. Consequently, the proposed embedding algorithm implies that our stego image has an excellent quality.

In our method, the embedded images include both the encrypted confidential image and two kinds of cheating image (i.e., meaningful and meaningless cheating images), which can raise the hacker's analysis costs efficiently. Only legal users having the correct random seed RS can distinguish between the encrypted confidential image and the cheating images. Additionally, the confidential image is encrypted by using the reliable cryptography methods (e.g., AES or RSA) before the embedding phase. These imply that the proposed method has good security.

2.2. Recovery and Extraction Phase.

When a legal user receives n stego images and the same random seed RS as in the embedding phase, the cover image can be restored by using the recovery algorithm. Then, the embedded messages, which include encrypted confidential images and cheating images, can be extracted by using the extraction algorithm. The extraction algorithm uses the random seed RS to generate the embedding order to distinguish confidential images from cheating images in extracted messages. The flowchart of the recovery and extraction method is shown in Fig. 3.

The recovery and extraction algorithm is described as follows.

Step 1. Calculate the difference $d'_{i,j}$ between the pixel with the position (i, j) of the first stego image and that of the last stego image, i.e., $d'_{i,j} = \hat{P}_{i,j}^1 - \hat{P}_{i,j}^n$

Step 2. Use the following two rules to recover the cover image and extract the embedded message $e_{i,j}^l$.
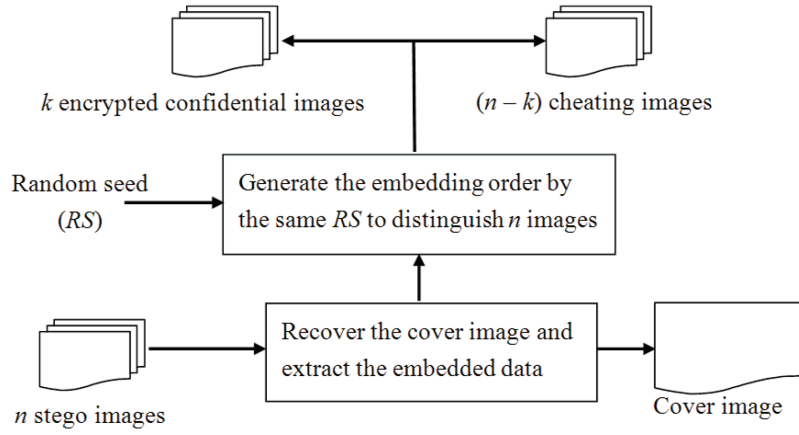
FIGURE 3. Flowchart of the recovery and extraction method

Rule 1. If $d'_{i,j} = 2$, then the cover pixel is recovered by using the equation
$P_{i,j} = (\sum_{l=1}^{n} \hat{P}_{i,j}^{l})/n$. In addition, the embedded messages $\{e_{i,j}^1, e_{i,j}^2, \ldots, e_{i,j}^n\}$,
which are equal to 1, can be extracted.

Rule 2. If $d'_{i,j} < 2$, the cover pixel is restored by using the equation
$P_{i,j} = \min_{1 \leq l \leq n} \left\{\hat{P}_{i,j}^l\right\}$. Moreover, the embedded message $e_{i,j}^l$ can be
extracted by using the equation

$$e_{i,j}^l = \begin{cases} 0, & if \ \ hatP_{i,j}^l = P_{i,j}, \\ 1, & if \ \ hatP_{i,j}^l > P_{i,j}. \end{cases}$$

Step 3. Use the same random seed RS to generate the embedding order of encrypted
confidential images and cheating images. Therefore, the encrypted confidential
images can be correctly identified according to the embedding order.

In the extraction and recovery phase, the cover pixel can be completely recovered if the
$\hat{P}_{i,j}^l$ that has embedded the message "0" is not lost. Once the cover pixel is recovered suc-
cessfully, the embedded message can be extracted correctly. Consequently, our proposed
method has good robustness.

2.3. **Solutions for Overflow and Underflow Problems.** In the embedding phase,
the pixel remains unchanged after the message "0" is embedded, which does not cause
the overflow and underflow problems. Otherwise, the pixel is modified by only increasing
or decreasing one for embedding the message "1". Therefore, an overflow or underflow
problem will occur due to the modification for the pixel that equals or 255. Inspired
by Lee and Huang's method [13], a mechanism is proposed to overcome this problem.
Since the proposed mechanism does not need a location map and extra messages, it can
maintain a high embedding rate. The proposed mechanism is described as follows.

In the embedding phase, the pixel with the location (i, j) does not embed any message
if any of the stego pixels $\left\{\hat{P}_{i,j}^1, \hat{P}_{i,j}^2, \ldots, \hat{P}_{i,j}^n\right\}$ has an overflow or underflow problem. In
order to identify these non-embeddable pixels, the pixel must be modified by using the
following equations

$$\hat{P}_{i,j}^l = P_{i,j}, l = 2, 3, ..., n, and$$

$$\hat{P}_{i,j}^1 \begin{cases} 3, & if \ \hat{P}_{i,j}^1 \leq 0, \\ 252, & if \ \hat{P}_{i,j}^1 \geq 255, \\ \hat{P}_{i,j}^1 & otherwise. \end{cases}$$

According to the above modification, it is obviously observed that the pixel with the location (i, j) is non-embeddable if the absolute difference between $\hat{P}_{i,j}^n$ and $\hat{P}_{i,j}^l$ is 3. Moreover, the cover pixel can be recovered by using the following equation $P_{i,j} = \min_{1 \leq l \leq n} \left\{ \hat{P}_{i,j}^l \right\}$.

3. **Experimental Results and Discussion.** We implemented our proposed method and six recently developed methods, which are proposed by Lee and Chen [11], Lee et al. [12], Lee and Huang [13], Ni et al. [18], Tseng and Hiseh [20] and Tai et al. [24], respectively. Fourteen test images, including ten nature images and four medical images, are shown in Fig. 4. We adopted the peak signal to noise ratio (PSNR) to measure the similarity of the stego image and the original image. Furthermore, the pure embedding rate (PER) is used to evaluate the hiding capacity of the proposed method. The equation of PER is

$$\text{PER} = \frac{HC - CI}{W \times H \times n}(bpp),$$

where HC denotes the number of the embeddable pixels; CI denotes the number of the cheating messages; W and H are the width and height of the test image, separately; and n is the number of the stego images. On the other hand, we use the equations

$$\text{ERC} = \frac{\text{Number of the correct extracted messages}}{HC - CI} \ and$$

$$\text{RCR} = \frac{\text{Number of the correct extracted messages}}{W \times H}$$

to measure the correct rates of the extracted message and the recovered pixel, respectively.

Table 2 lists the performance of the proposed method in theory. Suppose that each pixel does not have an overflow or underflow problem. Since each pixel can embed one message, the ideal pure embedding rate is 1. Assume that all embedded messages are 0. The stego image is the same as the cover image because the proposed method does not modify any pixel. In other words, the stego image is lossless. However, in general, the embedded messages have a 50% probability of being "0" and a 50% probability of being "1". In this case, half of the pixels in the image are modified by adding or decreasing one. According to the above modification, the value of the excepted PSNR is 51.14 dB.

Assume that each pixel in every stego image has an overflow or underflow problem. In order to solve the problem, each pixel in the first stego image must be added or decreased by 3. After the modifying procedure, each stego image is the same as the cover image except the first stego image, the quality of which is decreased to 38.58 dB. However, the difference between the first stego image and the cover image is small, which cannot be detected by the third party.

Tables 3, 4, 5, and 6 show the experimental results of the proposed method with different parameters (k, n). The experimental results show that ten nature images have an advantage over four medical images since they have higher embedding rate and better image quality. This is due to the fact that there are fewer extreme pixels in the nature image than in the medical image. The extreme pixel may easily cause an overflow or underflow problem, thereby decreasing both the image quality and hiding capacity. Nevertheless, the quality of the image which has the most extreme pixels is higher than 44 dB by using the proposed method.

TABLE 2. Performance analysis of the proposed method

Ideal PER (bpp)	Best PSNR (dB)	Expected PSNR (dB)	Worst PSNR (dB)
1	lossless	51.14	38.58

TABLE 3. Experimental results of the (2, 2)-images method

Image	Pure embedding rate	SIQ-1	SIQ-2
Lena	1	51.14	51.14
Baboon	1	51.14	51.15
Barbara	1	51.13	51.13
Pepper	1	51.14	51.14
Girl	1	51.12	51.13
Boat	1	51.14	51.14
Goldhill	1	51.15	51.14
Sailboat	1	51.14	51.14
Tiffany	1	51.13	51.13
Zelda	1	51.15	51.13
Medical image 1	0.80	44.88	52.96
Medical image 2	0.84	45.78	52.71
Medical image 3	0.83	45.47	52.86
Medical image 4	0.79	44.79	53.46

SIQ: stego image quality

TABLE 4. Experimental results of the (3, 3)-images method

Image	Pure embedding rate	SIQ-1	SIQ-2	SIQ-3
Lena	1	51.14	52.39	51.14
Baboon	1	51.15	52.38	51.13
Barbara	1	51.14	52.40	51.12
Pepper	1	51.13	52.38	51.14
Girl	1	51.15	52.38	51.14
Boat	1	51.14	52.37	51.13
Goldhill	1	51.15	52.37	51.13
Sailboat	1	51.13	52.40	51.14
Tiffany	1	51.13	52.38	51.13
Zelda	1	51.14	52.37	51.13
Medical image 1	0.84	45.61	52.93	52.24
Medical image 2	0.92	47.67	52.39	51.84
Medical image 3	0.91	47.31	52.42	51.95
Medical image 4	0.89	46.91	52.38	52.14

Figs. 5 (a)-(d) display the comparison results among the proposed method and six recently developed methods in [11, 12, 13, 18, 20, 24]. The pure embedding rates of our proposed method and that of three DE-based methods in [11, 12, 24] approach 1 bpp. However, three DE-based methods embed the confidential message by the expanded difference, thereby reducing the image quality. Unlike DE-based methods, our proposed

FIGURE 4. Fourteen test images with size of 512×512

method modifies the cover pixel by increasing and subtracting one. Consequently, the image quality of our proposed method is superior to that of three DE-based methods.

Both the pure embedding rate and the image quality of our proposed method are higher than those of Ni et al.'s method [18]. This is because the embeddable pixel that equals to peak point P embeds only one message in Ni et al.'s method. All embeddable pixels and non-embeddable pixels must be modified. Unlike Ni et al.'s method, only the embeddable pixels must be added or decreased by one to embed confidential message in our method.

Different modification approaches of pixels determine that the image quality and the hiding capacity of the proposed method are better than those of Ni et al.'s method.

Although the pure embedding rate of Lee and Huang's method is 1.07 bpp, which is greater than that of our method, the image quality of our method is 51.13 dB, which is higher than that of their method. Additionally, the proposed method can cheat hackers or immensely increase their analysis cost.

TABLE 5. Experimental results of the (4, 4)-images method

Image	Pure embedding rate	SIQ-1	SIQ-2	SIQ-3	SIQ-4
Lena	1	51.13	51.74	51.71	51.13
Baboon	1	51.13	51.70	51.72	51.14
Barbara	1	51.14	51.73	51.71	51.13
Pepper	1	51.14	51.71	51.72	51.14
Girl	1	51.14	51.72	51.70	51.13
Boat	1	51.15	51.70	51.71	51.13
Goldhill	1	51.14	51.71	51.72	51.15
Sailboat	1	51.12	51.72	51.72	51.13
Tiffany	1	51.14	51.71	51.72	51.13
Zelda	1	51.15	51.71	51.73	51.14
Medical image 1	0.86	46.07	52.24	52.22	51.93
Medical image 2	0.96	49.09	51.71	51.72	51.48
Medical image 3	0.95	48.65	51.74	51.75	51.54
Medical image 4	0.94	48.54	51.71	51.72	51.62

TABLE 6. Experimental results of the (5, 5)-images method

Image	Pure embedding rate	SIQ-1	SIQ-2	SIQ-3	SIQ-4	SIQ-5
Lena	1	51.13	51.43	51.41	51.42	51.13
Baboon	1	51.12	51.42	51.42	51.42	51.15
Barbara	1	51.13	51.42	51.42	51.43	51.12
Pepper	1	51.13	51.42	51.42	51.43	51.14
Girl	1	51.14	51.42	51.40	51.41	51.15
Boat	1	51.13	51.42	51.42	51.42	51.14
Goldhill	1	51.15	51.43	51.40	51.41	51.13
Sailboat	1	51.13	51.43	51.41	51.42	51.13
Tiffany	1	51.15	51.41	51.43	51.42	51.13
Zelda	1	51.14	51.42	51.43	51.42	51.13
Medical image 1	0.87	46.27	51.93	51.94	51.93	51.78
Medical image 2	0.98	49.99	51.42	51.42	51.43	51.31
Medical image 3	0.97	49.49	51.45	51.46	51.46	51.34
Medical image 4	0.97	49.62	51.42	51.42	51.42	51.37

These above merits can be illustrated by the following example with $k = 1$ and $n = 3$. Fig. 6 (a) shows a cover image; Fig. 6 (b) presents an encrypted confidential image; and both Figs. 6 (c)-(d) illustrate two cheating images, in which Fig. 6 (c) contains meaningful messages while Fig. 6 (d) contains meaningless messages. The ID numbers of Figs. 6 (b)-(d) are 1, 2, and 3, respectively. In all traditional methods mentioned in Section 1, the order of embedding Figs. 6 (b)-(d) into stego images conforms to their

ID numbers. However, our method uses a random seed RS to generate an embedding order in the embedding phase. Assume that the embedding order is {3, 2, 1} According to the embedding order and the embedding rules, Fig. 6 (d) is embedded into the first stego image (i.e., Fig. 6 (e)), Fig. 6 (c) is embedded into the second stego image (i.e., Fig. 6 (f)), and Fig. 6 (b) is embedded into the third stego image (i.e., Fig. 6 (g)). Although the third party can extract all embedded messages (i.e., Figs. 6 (b)-(d)) by using our recovery and extraction algorithm, he/she cannot identify which figure contains the encrypted confidential messages without knowing the embedding order.

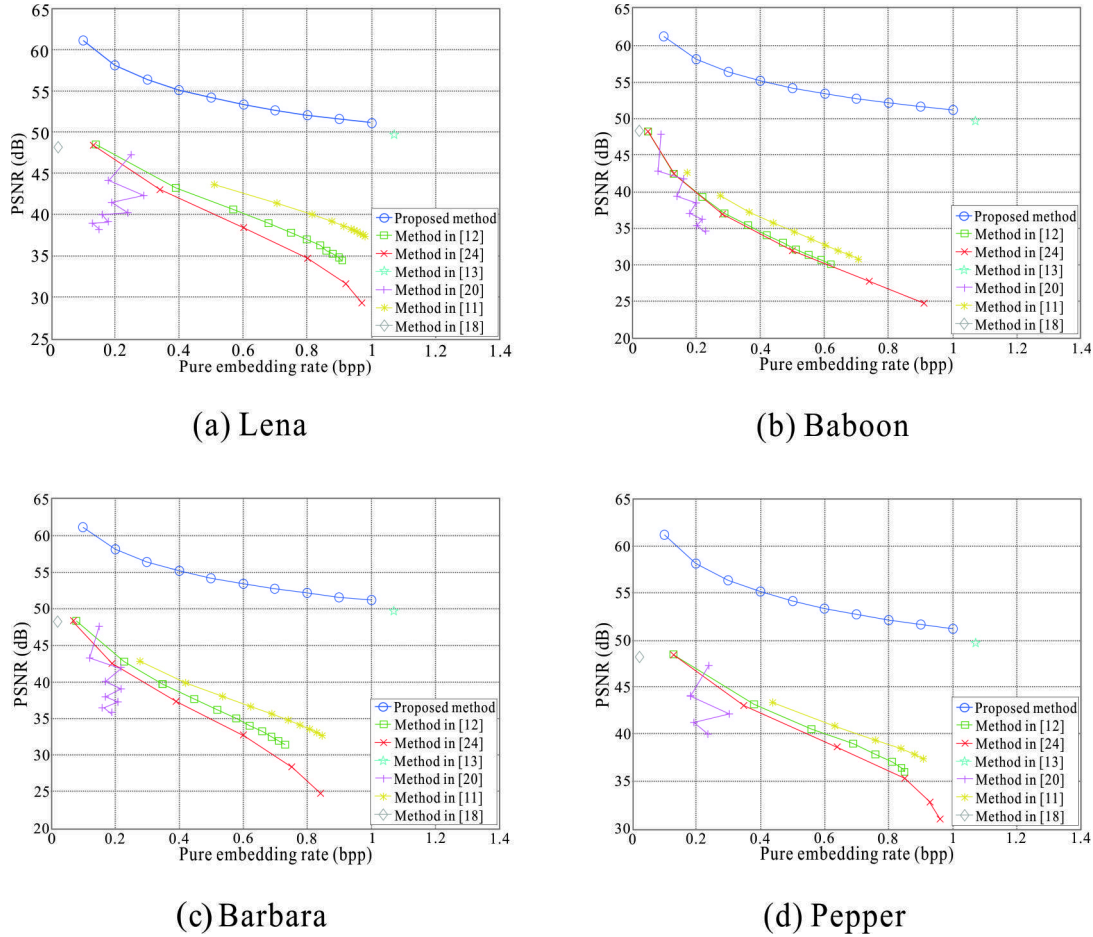(a) Lena

(b) Baboon

(c) Barbara

(d) Pepper

FIGURE 5. Comparison results among the proposed method and six recently developed methods in [11, 12, 13, 18, 20, 24]

Figs. 7 (a)-(b) show the robustness of the proposed method with different values of parameter n. The correct rates of the extracted message and the recovered pixel are high even if two stego images are lost. Additionally, most pixels can be recovered successfully if the parameter n is greater than 14. This implies that the suitable parameter n should be greater than 14, which can achieve the robustness.

4. **Conclusions.** In our (k, n)-image reversible data hiding method, the cover image and the confidential message can be successfully recovered from n stego images. Most cover pixels and confidential messages can be correctly restored when some stego images are lost. Consequently the proposed method achieves good robustness. Since the embeddable pixel can embed one message by adding or subtracting one, the visual difference between the cover image and the modified image is pretty small. It is indicated that the image quality obtained by our method is excellent.
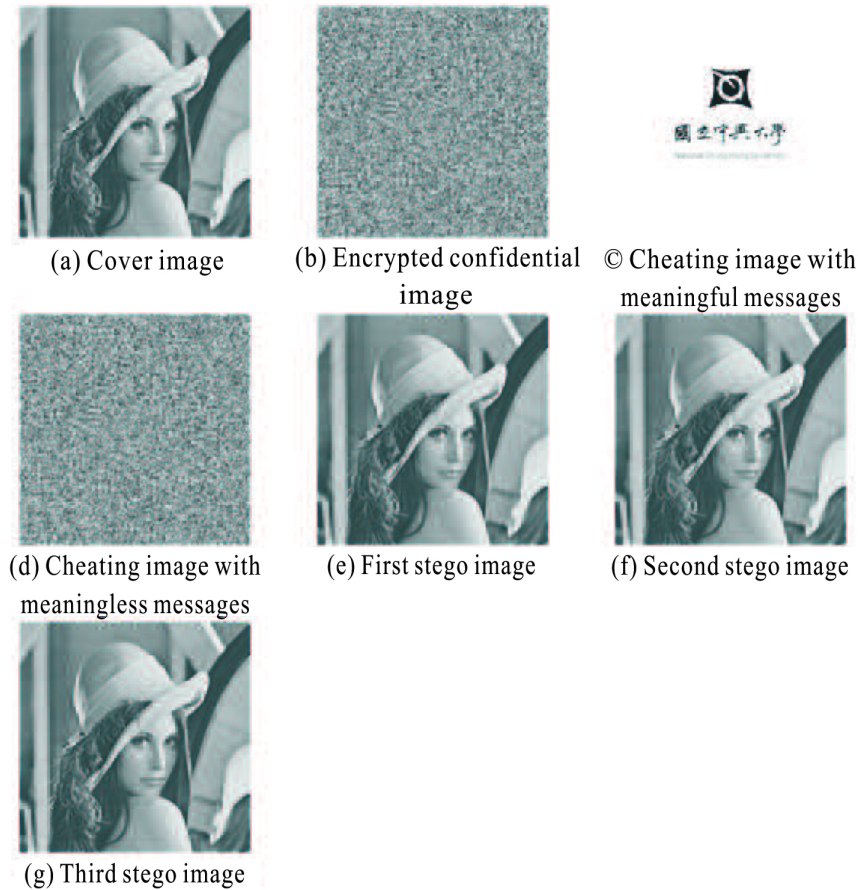
(a) Cover image

(b) Encrypted confidential image

© Cheating image with meaningful messages

(d) Cheating image with meaningless messages

(e) First stego image

(f) Second stego image

(g) Third stego image

FIGURE 6. A cheating example of the proposed method

(a) Correct rate of the recovered pixel
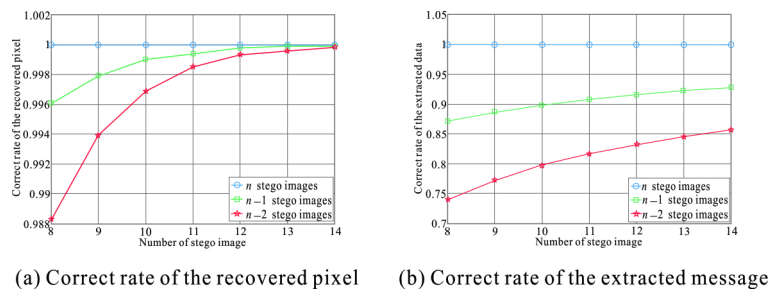
(b) Correct rate of the extracted message

FIGURE 7. Robustness of the proposed method

(k, n)-image reversible data hiding method can embed k confidential images and $(n-k)$ cheating images to deceive hackers or increase their analysis cost. This implies that the proposed method owns the property of security. Experimental results prove that the proposed method is better than recently developed methods.

Although the proposed method does not record any extra data or location map, the modification level of the pixel in the first image is large. In the future, we will try to add the concept of the pairwise difference adjustment method [25] into the proposed method, thereby reducing image distortion.

REFERENCES

[1] A. M. Alattar, Reversible watermark using the difference expansion of a generalized integer transform, *IEEE Trans. Image Processing*, vol. 13, no. 8, pp. 1147-1156, 2004.

[2] D. Coltuc, and J. M. Chassery, Very fast watermarking by reversible contrast mapping, *Journal of IEEE Signal Processing Letters*, vol. 14, no. 4, pp. 255-258, 2007.

[3] Y. K. Chan, W. T. Chen, S. S. Yu, Y. A. Ho, C. S. Tsai, and Y. P Chu, A HDWT-based reversible data hiding, *Journal of Systems and Software*, vol. 82, no. 3, pp. 411-421, 2009.

[4] C. C. Chang, T. D. Kieu, and Y. C. Chou, Reversible data hiding scheme using two steganographic images, *Proc. IEEE Region 10 Conference TENCON*, pp. 1-4, 2007.

[5] M. U. Celik, G. Sharma, A. M. Tekalp, and E. Saber, Lossless generalized-LSB data embedding, *IEEE Trans. Image Processing*, vol. 14, no. 2, pp. 253-266, 2005.

[6] M. Fallahpour, D. Megias, and M. Ghanbari, Reversible and high-capacity data hiding in medical images, *Journal of IET Image Processing*, vol. 5, no. 2, pp. 190-197, 2011.

[7] W. Hong, Adaptive reversible data hiding method based on error energy control and histogram shifting, *Journal of Optics Communications*, vol. 285, no. 2, pp. 101-108, 2012.

[8] W. Hong, and T. S. Chen, Reversible data embedding for high quality images using interpolation and reference pixel distribution mechanism, *Journal of Visual Communication and Image Representation*, vol. 22, no. 2, pp. 131-140, 2011.

[9] W. Hong, T. S. Chen, and C. W. Shiu, Reversible data hiding for high quality images using modification of prediction error, *Journal of Systems and Software*, vol. 82, no. 11, pp. 1833-1842, 2009.

[10] Y. Hu, H. K. Lee, and J. Li, DE-based reversible data hiding with improved overflow location map, *IEEE Trans. Circuits and Systems for Video Technology*, vol. 19, no. 2, pp. 250-260, 2009.

[11] C. F. Lee, and H. L. Chen, Adjustable prediction-based reversible data hiding, *Journal of Digital Signal Processing*, vol. 22, no. 6, pp. 941-953, 2012.

[12] C. F. Lee, H. L. Chen, and H. K. Tso, Embedding capacity raising in reversible data hiding based on prediction of difference expansion, *Journal of Systems and Software*, vol. 83, no. 10, pp. 1864-1872, 2010.

[13] C. F. Lee and Y. L. Huang, Reversible data hiding scheme based on dual stegano-images using orientation combinations, *Journal of Telecommunication Systems*, vol. 52, no. 4, pp. 2237-2247, 2013.

[14] T. C. Lu and Y. H. Huang, An effective lossless hiding technique based on reversible contrast mapping and histogram embedding methods, *Proc. of the 5th International Conference on Information Assurance and Security*, pp. 299-602, 2009.

[15] C. F. Lee, K. H. Wang, C. C. Chang, and Y. L. Huang, A reversible data hiding scheme based on dual steganographic images, *Proc. of the 3rd International Conference on Ubiquitous Information Management and Communication*, pp. 228-237, 2009.

[16] Y. C. Liu, H. C. Wu, and S. S. Yu, Adaptive DE-based reversible steganographic technique using bilinear interpolation and simplified location map, *Journal of Multimedia Tools and Applications*, vol. 52, no. 2-3, pp. 263-276, 2011.

[17] Y. C. Li, C. M. Yeh, and C. C. Chang, Data hiding based on the similarity between neighboring pixels with reversibility *Journal of Digital Signal Processing*, vol. 20, no. 4, pp. 1116-1128, 2009.

[18] Z. Ni, Y. Q. Shi, N. Ansari, and W. Su, Reversible data hiding, *IEEE Trans. Circuits and Systems for Video Technology*, vol. 16, no. 3, pp. 354-362, 2006.

[19] J. Tian, Reversible data embedding using a difference expansion, *IEEE Trans. Circuits and Systems for Video Technology*, vol. 13, no. 8, pp. 890-896, 2003.

[20] H. W. Tseng, and C. P Hsieh, Prediction-based reversible data hiding, *Journal of Information Sciences* vol. 179, no. 14, pp. 2460-2469, 2009.

[21] P. Tsai, Y. C. Hu, and H. L. Yeh, Reversible image hiding scheme using predictive coding and histogram shifting, *Journal of Signal Processing*, vol. 89, no. 6, pp. 1129-1143, 2009.

[22] D. M. Thodi, and J. J. Rodriguez, Expansion embedding techniques for reversible watermarking, *IEEE Trans. Image Processing*, vol. 16, no. 3, pp. 721-730, 2007.

[23] D. M. Thodi and J. J. Rodriguez, Prediction-error based reversible watermarking, *Proc. of International Conference on Image Processing*, pp. 1549-1552, 2004.

[24] W. L. Tai, C. M. Yeh, and C. C. Chang, Reversible data hiding based on histogram modification of pixel differences, *IEEE Trans. Circuits and Systems for Video Technology*, vol. 19, no. 6, pp. 906-910, 2009.

[25] S. Weng, Y. Zhao, J. S. Pan, and R. Ni, Reversible watermarking based on invariability and adjustment on pixel pairs, *Journal of IEEE Signal Processing Letters*, vol. 15, pp. 721-724, 2008.

[26] H. W. Yang, I. E. Liao, and C. C. Chen, Reversible data hiding based on median difference histogram, *Journal of Information Science and Engineering*, vol. 27, no. 2, pp. 577-293, 2011.

[27] Z. F. Zhao, H. Luo, Z. M. Lu, and J. S. Pan, Reversible data hiding based on multilevel histogram modification and sequential recovery, *International Journal of Electronics and Communications*, vol. 65, no. 10, pp. 814-826, 2011.

[28] X. T. Zeng, Z. Li, and L. D. Ping, Reversible data hiding scheme using reference pixel and multilayer embedding, *International Journal of Electronics and Communications*, vol. 66, no. 7, pp. 532-539, 2012.